808-nm Optical Parametric Amplification Based on DKDP Crystals

Liang Xiao[1,2] Kang Jun[2] Sun Meizhi[2] Xie Xinglong[2] Zhu Jianqiang[2]

[1] *Department of Physics, College of Sciences, Shanghai University, Shanghai* 200444, *China*

[2] *Key Laboratory of High Power Laser and Physics, Shanghai Institute of Optics and Fine Mechanics, Chinese Academy of Sciences, Shanghai* 201800, *China*

Abstract The optical parametric chirped pulse amplification (OPCPA) near the 800 nm wavelength has gained significant popularity in the recent years. This can be attributed to the development of laboratory-scale Nd:glass lasers with their associated second harmonic generation (SHG), the mature nonlinear crystal growth technology, and the commercialized mode-locked Ti:sapphire oscillator. In this study, the characteristics of the 808-nm centered broad bandwidth signal OPCPA based on potassium dideuterium phosphate (DKDP) crystals are investigated. The phase mismatch in DKDP crystals for different deuteration levels of 0～99% is studied and a numerical simulation of the high energy optical parameric amplification (OPA) process with the considerations of absorption and several high deuteration levels is presented. Results show that the broadband bandwidth OPCPA at 808 nm can be obtained when the deuteration level is more than 90%.

Key words nonlinear optics; 808-nm optical parametric chirped pulse amplification; deuteration; potassium dideuterium phosphate; phase mismatch

OCIS codes 190.4970; 160.4330; 140.4480

基于 DKDP 晶体的 808 nm 波段光参量放大研究

梁 潇[1,2] 康 俊[2] 孙美智[2] 谢兴龙[2] 朱健强[2]

[1] 上海大学理学院物理系，上海 200444

[2] 中国科学院上海光学精密机械研究所高功率激光物理联合实验室，上海 201800

摘要 近年来，在 800 nm 波段进行光参量啁啾脉冲放大(OPCPA)的实验受到了极大的关注，这得益于大口径高能钕玻璃激光装置及其倍频技术(SHG)的逐渐成熟，非线性晶体生长技术的发展，以及钛宝石锁模飞秒激光器的商业化。理论分析了基于氘化磷酸二氢钾(DKDP)的 808 nm 波段宽带光参量啁啾脉冲放大现象。具体分析了 DKDP 晶体的氘化率从 0 提高至 99%时的相位失配情况，并且在考虑光吸收情况下，数值模拟了几种高氘化率 DKDP 晶体的大能量光参量放大(OPA)过程。结果表明，大于 90%氘化率的 DKDP 晶体在 800 nm 波段可实现宽带 OPCPA。

关键词 非线性光学；808 nm 光参量啁啾脉冲放大；氘化率；磷酸二氢钾；相位失配

中图分类号 O437.4；TN242 **文献标识码** A

doi：10.3788/LOP53.081901

1 Introduction

Optical parametric chirped pulse amplification (OPCPA) pumped by the second harmonic generation (SHG) of Nd:glass lasers is presently the most promising method to produce ultra-intense pulses ($>10^{23}$ W·cm^{-2}) that can be used to study extreme relativistic phenomena[1]. Owing to the large aperture of potassium dihydrogen phosphate

收稿日期：2016-05-01；**收到修改稿日期**：2016-05-12；**网络出版日期**：2016-07-27

基金项目：国家自然科学基金(11304332)

作者简介：梁 潇(1990—)，男，硕士研究生，主要从事光参量啁啾脉冲放大技术方面的研究。E-mail：lx62@siom.ac.cn

导师简介：朱健强(1964—)，男，博士，研究员，博士生导师，主要从事高功率激光器设计等方面的研究。E-mail：jqzhu@mail.shcnc.ac.cn

(KDP) and potassium dideuterium phosphate (DKDP), the Vulcan 10 PW laser project in UK aims to create a source of 30-fs laser pulses with a 300-J energy and the intensity up to 10^{23} W·cm^{-2} based on OPCPA. A similar project, named PEARL-10, is being implemented in Russia with the objective of creating a source of 20-fs laser pulses with energy exceeding 200 J and the maximum intensity over 10^{23} W·cm^{-2} [2-3]. Further, the LLE in USA is developing a high-energy optical parametric amplifier line (OPAL) pumped by the SHG of OMEGA EP with the planned focal intensity up to 10^{24} W·cm^{-2} and the peak power up to 200 PW[4]. For the above petawatt-level lasers, the 910-nm centered signal is selected to be amplified because it has been shown that the DKDP can offer 190-nm gain bandwidths around this wavelength[5-6]. Meanwhile, many other high-quality crystals such as the LBO, BBO, and YCOB have been studied for optical parametric amplification (OPA)[7-11]. When compared with the DKDP, these three types of nonlinear crystals have much higher nonlinear coefficients and broader gain bandwidths in the visible and near infrared spectral ranges.

Therefore, we assume an ultra-intense laser amplification chain based on OPCPA which uses LBO, BBO, or YCOB crystals as the nonlinear gain media, and an 808-nm centered signal is selected. The 808 nm wavelength corresponds to the maximum spectrum of our oscillator, and there are some advantages to the OPA using signals near 800 nm. Compared to 900-nm centered systems, the 800-nm centered system has a more convenient splitting ratio between signal and idler photon energy. This could lead to a higher efficiency in the 800-nm centered systems. Further, shorter pulses can be obtained with the same wavelength bandwidth when the central wavelength is shorter. Meanwhile, the commercial Ti∶sapphire oscillators are a quite stable and mature front-end to provide ultra-broadband 808-nm centered signals. A stretcher will be used after the oscillator to broaden the pulse width of the signal to nanoseconds and its energy will subsequently be amplified to hundreds of joules by the OPA chain. However, in recent reports of OPCPA experiments[12-13], the largest sizes of LBO and YCOB crystals used are 100 mm and 63 mm, respectively. Considering the substantial loss of the compressor, the damage thresholds of nonlinear crystals and optical element film layers, the diameters of the main OPA at the last stage in such ultra-intense laser facility need to be larger than several hundred millimeters to support ultra-short pulses of hundreds of joules. Under this condition, the three types of crystals are still not yet suitable for the main final OPA , and the DKDP becomes attractive for the OPA of such systems, as it can be grown in sizes larger than 400 mm in aperture. Considering the grating size of the compressor and its energy threshold for the current technology of compression[4], a 4500-J output energy of the final amplifier with 400-mm DKDP can be appropriate, and the laser pulse peak power after compression will be 90 PW, with a pulse width of 30 fs.

Our study contains detailed analysis of the utilization of DKDP crystal in OPA centered at 808 nm. First, we analyze the OPA parametric bandwidth by studying the wave vector mismatch in DKDP of different deuteration levels. Then, we present a numerical simulation of type I OPA based on DKDP crystal and attempt to identify the maximal gain bandwidth by making flexible use of the zero phase mismatch wavelength (ZPMW). In addition, the absorption in the infrared (IR) region for DKDP of different deuteration levels is another important factor for the OPCPA efficiency[14], and it will be studied in this work. All the theoretical analysis and numerical simulations refer to the signal pulse of center wavelength at 808 nm from a Ti∶sapphire oscillator and the pump pulse of 526.5 nm wavelength from the SHG of the Nd∶glass laser.

2 Wave vectors mismatch analysis around 808 nm in DKDP

Wave vector match geometry is significantly important to OPA because it affects the energy gain and bandwidth of the OPA spectrum. For the uniaxial nonlinear crystal DKDP, type I noncollinear phase-matching geometry is

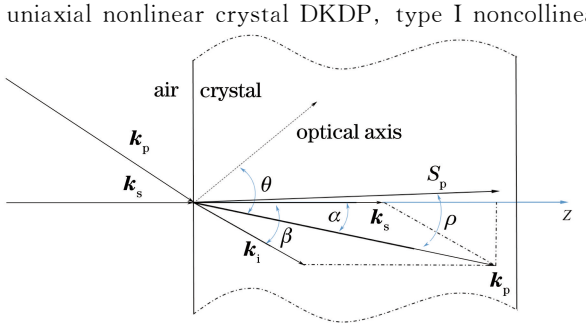

Fig. 1 Schematics of Type I noncollinear phase-matching geometry inside the crystal

used in our analysis, as presented in Fig. 1. θ is the phase-matching angle of the pump relative to the optical axis. The noncollinear angle α between the pump wave vector $\boldsymbol{k}_{\mathrm{p}}$ and the signal wave vector $\boldsymbol{k}_{\mathrm{s}}$ is compensated by the pump walk-off angle ρ. β is the noncollinear angle between wave vector $\boldsymbol{k}_{\mathrm{s}}$ and idler wave vector $\boldsymbol{k}_{\mathrm{i}}$. This type of phase-matching geometry is called Poynting vector walk-off compensation, which results in less asymmetry in the spatial beam profile and a better stability gain during the OPCPA process[15].

Based on the schematic shown in Fig. 1 and the conservation of energy and momentum, the wave vector mismatch equations produced by the crystal DKDP at different deuteration levels is derived as

$$\Delta k = 2\pi\left[\frac{n_{\mathrm{e,p}}(D,\theta)}{\lambda_{\mathrm{p}}}\cos\alpha - \frac{n_{\mathrm{o,s}}(D,\lambda_{\mathrm{s}})}{\lambda_{\mathrm{s}}} - \frac{n_{\mathrm{o,i}}(D,\lambda_{\mathrm{i}})}{\lambda_{\mathrm{i}}}\cos\beta\right], \tag{1}$$

$$\beta = \alpha + \arcsin\left[n_{\mathrm{o,s}}\lambda_{\mathrm{i}}\sin\alpha/(n_{\mathrm{o,i}}\lambda_{\mathrm{s}})\right], \tag{2}$$

where the subscripts o, e, p, s, and i stand for ordinary light, extraordinary light, pump, signal, and idler, respectively. D represents the deuteration level. Equation (1) considers only the parallel part of the wave vector mismatch. We consider the match in the signal vector direction and neglect the group-velocity mismatch (GVM)[8]. It can be seen that the refractive index of each wavelength in the crystal is the key variable to determine the wave vector mismatch Δk. For DKDP crystal, according to Ref. [5], the refractive index, which depends on the wavelength and deuteration level, can be written in the form

$$n^2_{\mathrm{o,e}}(D,\lambda) = \left[\frac{n^2_{\mathrm{o,e}}(0.96,\lambda) - 0.04n^2_{\mathrm{o,e}}(0,\lambda)}{0.96}\right]D + (1-D)\,n^2_{\mathrm{o,e}}(0,\lambda), \tag{3}$$

where $n^2_{\mathrm{o,e}}(0.96,\lambda)$ and $n^2_{\mathrm{o,e}}(0,\lambda)$ are defined as

$$n^2_{\mathrm{o,e}}(\lambda) = A_{\mathrm{o,e}} + \frac{B_{\mathrm{o,e}}}{\lambda^2 - C_{\mathrm{o,e}}} + \frac{F_{\mathrm{o,e}}\lambda^2}{\lambda^2 - E_{\mathrm{o,e}}}. \tag{4}$$

The specific values of each coefficients are listed in the following table.

Table 1 Coefficient value of equation (4)

Deuteration	Polarization	A	B	C	F	E
$D=0$	o	2.259276	10.089562	1.2942625	13.00522	400
$D=0$	e	2.132668	8.637494	1.2281043	3.2279924	400
$D=0.96$	o	2.240921	9.676393	1.5620153	2.2469564	126.920659
$D=0.96$	e	2.126019	8.578409	1.1991324	0.7844043	123.403407

The validity of equation (3) has been justified in Ref. [6]. Their experiments show a good agreement with simulations that contain the refractive index equations (3) and (4) in their codes.

It should be noted that we can calculate the phase-matching angle θ in Fig. 1 by solving equations (1) and (2), and the result is equation (5). The phase-matching angle equation that will be used throughout our study.

$$\theta_{\mathrm{m}} = \arcsin\left\{\left[\frac{\dfrac{n^2_{\mathrm{o,p}}}{\lambda^2_{\mathrm{p}}} - \left(\dfrac{n_{\mathrm{o,s}}}{\lambda_{\mathrm{s}}} + \dfrac{n_{\mathrm{o,i}}}{\lambda_{\mathrm{i}}}\cos\beta\right)^2 \Big/ \cos^2\alpha}{n^2_{\mathrm{o,p}} - n^2_{\mathrm{e,p}}}\right]^{1/2} \times \frac{n_{\mathrm{e,p}}\cos\alpha}{\dfrac{n_{\mathrm{o,s}}}{\lambda_{\mathrm{s}}} + \dfrac{n_{\mathrm{o,i}}}{\lambda_{\mathrm{i}}}\cos\beta}\right\}. \tag{5}$$

The phase mismatch of each wavelength is fixed after the wave vector mismatch has been selected.

$$\Delta\varphi(\lambda_{\mathrm{s}}) = \Delta k(\lambda_{\mathrm{s}}) \times L, \tag{6}$$

where L (constant) is the crystal length, and the phase mismatch differs only from the signal wavelength. The gain of certain wavelengths will be much smaller (drop to zero in a sinc function) if their phase mismatch $\Delta\varphi$ is larger than π[8], and neither pump depletion nor initial idler beam is assumed here. We can define a region $|\Delta k(\lambda)| \leqslant \pi/L$ to describe the parametric bandwidth, under the condition that the perfect phase match is achieved at the center wavelength of the signal. The parametric bandwidth characteristics of different deuteration levels DKDP are presented in Fig. 2 which shows the curves of wave vector mismatch against the signal wavelength in 30-mm DKDP (30-mm long crystal corresponding to the highest conversion efficiency). The zero phase mismatch wavelength has been set at 808 nm, the pump wavelength is 526.5 nm, and the idler wavelength is 1511.2 nm. The blue lines in Figs. 2(a) and (b) are the mismatch curves at various deuteration levels of 10%~80%, with noncollinear angles of 0° and 0.5°, respectively (the 0.5° angle is selected because the distinct influence of the noncollinear angle on the parametric bandwidth between low and high deuteration levels can be obviously distinguished). Whether

there is a noncollinear angle or not, these wave mismatch lines vary abruptly around 808 nm, resulting in a large mismatch in a narrow interval between $\pm\pi/L$. Therefore, the parametric bandwidth will be less than 20 nm. According to the Fourier transform law, the DKDP of deuteration levels under 80% does not satisfy the compression bandwidth requirements for tens of femtoseconds (fs). Nevertheless, the results are improved when the deuteration level is higher than 85%. We calculate the mismatch curves at deuteration levels of 85%, 90%, 93%, 96%, and 99%, and the respective results are shown in Figs. 2(c) and (d). Apparently, the interval between $\pm\pi/L$ is much larger than that obtained at low deuteration levels, resulting in a larger parametric bandwidth. The results also highlight the importance of the noncollinear angle. When comparing Figs. 2(c) and (d), we find that while α increases to 0.5°, the wave vector mismatch curve rotates clockwise, centered at 808 nm. Thus, by controlling the noncollinear angle, we can modulate the mismatch, and therefore, the curve will be symmetric at the center of 808 nm and the mismatch is small for wavelengths around 808 nm. Both short and long wavelengths obtain an equivalent sufficient gain after amplification, which is beneficial to the time waveform of a linear chirped signal pulse and the largest gain bandwidth.

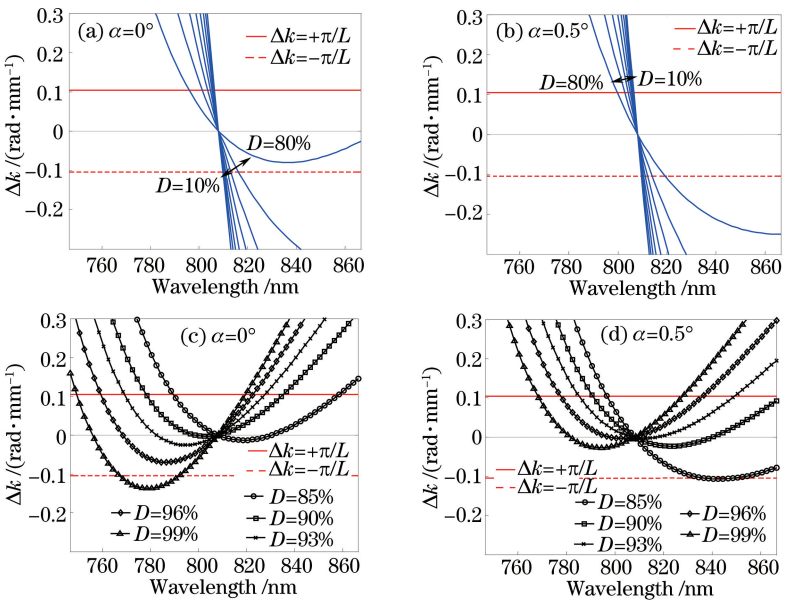

Fig. 2 Wave vector mismatch in DKDP centered at 808 nm. (a) Deuteration levels from 10% to 80%, noncollinear angle $\alpha=0°$; (b) deuteration levels from 10% to 80%, noncollinear angle $\alpha=0.5°$; (c) deuteration levels from 85% to 99%, noncollinear angle $\alpha=0°$; (d) deuteration levels from 85% to 99%, noncollinear angle $\alpha=0.5°$

Actually, the best noncollinear angle corresponds to the extreme phase-matching curve, and it is determined by specific situations, such as the amplified spectrum simulation in the OPCPA process when the absorption in the IR region and the pump depletion are considered. Therefore, in order to gauge the maximum possible amplified spectrum bandwidth with the best noncollinear angle, we should simulate the OPA process by solving the coupled wave equations.

3 Spectrum amplification analysis

In many parameter designs of petawatt laser systems, the energy of the final pulse is on the order of hundreds of joules, and the pulse width compressed is tens of femtoseconds to realize petawatt power. For example, for an ultra-short high-power OPCPA laser with the final power of 5 PW, the signal pulse should be amplified to 150 J, and a 30-fs pulse width is needed. Assuming that the chirp ratio of the compressor is −28 ps/nm, a 60-nm amplified bandwidth signal after the final main OPA would be suitable to be compressed near 30 fs. Based on the above parametric bandwidth analysis, the OPA bandwidth of low deuteration level DKDP is clearly unsatisfied. Whereas the bandwidth of high-deuterated DKDP is possible, we numerically simulate the 85%, 90%, 95%, and 99% deuteration levels OPA by solving the following coupled wave equations.

$$\frac{\partial A_s}{\partial z}=-\frac{j\omega_s d_{eff}}{n_s c}A_i^* A_p \exp(-j\Delta k z)-a_s A_s, \tag{7}$$

$$\frac{\partial A_i}{\partial z}=-\frac{j\omega_i d_{eff}}{n_i c}A_s^* A_p \exp(-j\Delta kz)-a_i A_i, \tag{8}$$

$$\frac{\partial A_p}{\partial z}=-\frac{j\omega_p d_{eff}}{n_p c\ \cos^2\rho}A_s A_i \exp(j\Delta kz)-a_p A_p, \tag{9}$$

where $A_{(s,i,p)}$ is the pulse amplitude, $\omega_{(s,i,p)}$ is the angular frequency, d_{eff} represents the effective nonlinear coefficient, c is the light speed, and z is the propagation distance. The last item on the right side refers to the absorption of DKDP: $a_{(s,i,p)}$ is the absorption coefficient, which is relative to deuteration level, wavelength, and transmission.

The transmittance data of the 95% deuteration level are shown in Fig. 3[14]. Signal and idler bands corresponding to the 808 nm central signal wavelength are marked out by the dotted lines. The idler wavelength is in the plunging area of transmittance, which indicates a strong absorption in the DKDP crystal. According to Ref. [14], the increasing of deuteration shifts the wavelength of the strong absorption further to the infrared, but the idler band is still covered in the range from 1362 nm to 1723 nm (pumped at 526.5 nm). To describe this relation between absorption and transmission we use the following equation.

$$a(\lambda,D)=-[\ln T(\lambda,D)]/2L_0, \tag{10}$$

where T represents the transmittance of L_0(1 cm) thick crystal. As the transmittance data is available only for the 95% deuteration level DKDP and the transmittance difference between other high deuteration levels (around 90%) should be very small, and we assume that the data are universally valid for all high deuteration, such as 85%, 90%, 95%, and 99%.

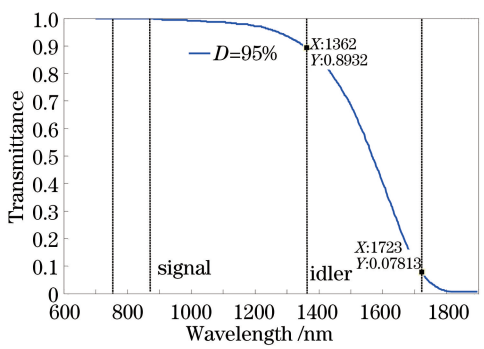

Fig. 3 Transmittance of a 1-cm thick DKDP crystal for different deuteration levels[14]

Equations (7-9) are the simplified coupled wave equations in which the walk-off effect in the spatial domain and the GVM in the time domain are not considered. Assuming there is no spatial chirp, the walk-off effect makes no difference in the spectrum gain of the OPA and the GVM effect can be neglected for nanosecond pulses OPA[16]. Some necessary parameters for numerical simulation are as follows: the effective nonlinear coefficient $d_{eff}=0.39\sin\theta\sin 2\varphi$ pm/V, where θ is the phase-matching angle and φ is the azimuthal angle which is equal to 45°. The spatial profiles of the incident signal and pump are both the top-hat shape, the temporal profiles are both the fourth super-Gaussian shape, $A(t)=\exp(t^4/2\tau_0^4)$, and their full widths at half maximum (FWHMs) are 2 ns and 2.2 ns, respectively. Certainly, the incident signal is a broadband pulse with a 20-fs pulse width from the Ti:sapphire oscillator; then the signal pulse width is stretchered to 2 ns due to the linear chirp (chirp rate 28 ps/nm) from the stretcher, and the corresponding FWHM of the signal bandwidth is 72 nm. The intensities of the incident 808-nm signal pulse and the 526.5-nm pump pulse are set as the following calculation. To obtain a multi-petawatt laser pulse, e.g., 30 fs, 150 J, the signal energy before compressor is about 250 J (60% diffraction efficiency in compressor) and the energy before the final amplification is 25 J. The intensity for a 125 mm×125 mm aperture, 2-ns pulse width signal is about 0.08 GW/cm^2. If the OPA conversion efficiency is 35%, the pump energy would be 700 J, and the intensity for a 125 mm×125 mm aperture, 2.2-ns pulse width pump pulse is about 2 GW/cm^2.

The impact of absorption on the OPA conversion efficiency for the complete signal spectrum in the 95% deuteration level DKDP is analyzed and presented in Fig. 4. The conversion efficiency is defined as the ratio between the amplified signal pulse energy and all of the incident pulses energy. The dotted line shows a little decline in conversion efficiency as the absorption is considered, but the OPA saturation length extends to 35 mm, where the largest conversion efficiency reaches 50%. It indicates that the pump energy can be converted to signal pulse effectively in a 35-mm long DKDP crystal, even if there is a strong idler absorption in the crystal. As for the other

high deuteration levels DKDP, the impact of absorption on the OPA is almost the same. Therefore, the amplified spectrum will be simulated in a 35-mm long DKDP for four deuteration levels under the consideration of absorption.

Fig. 5 shows the simulation results of amplified spectrum bandwidth FWHM at deuteration levels of 85%, 90%, 95%, and 99%. The phase-matching angle θ is set to perfectly match the signal center wavelength 808 nm for each noncollinear angle and deuteration. There are four best noncollinear angles to maximize the amplified bandwidth FWHMs, which are 62 nm (85%, 0°), 63 nm (90%, 0.44°), 63 nm (95%, 0.62°), and 64 nm (99%, 0.74°). These angles have already satisfied the 30-fs compression bandwidth requirement. However, the difference of the largest FWHM between these four deuteration levels is very small, which indicates that increasing the deuteration level to more than 90% does not significantly improve the bandwidth in this 808-nm phase-matching case, even if the noncollinear phase-matching geometry is used. Compared to the FWHM of the incident signal bandwidth (72 nm), the FWHM of amplified spectrum bandwidth decreases for all the four deuteration levels. This is because the phase mismatch of the wavelengths at the edge of the spectrum increases heavily and they cannot extract energy from the pump efficiently. If there is a method to decrease the phase mismatch of these wavelengths, the bandwidth of the amplified spectrum can be increased. In addition, as this simulation is specific to the energy amplification of OPA stage, the incident energy of the signal can be tens of joules, and the total signal gain after amplification is about 16 for all the four deuteration cases.

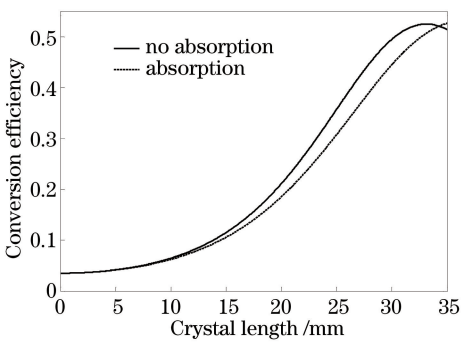

Fig. 4 Conversion efficiency with and without absorption in the OPA process with the 95% deuteration level DKDP

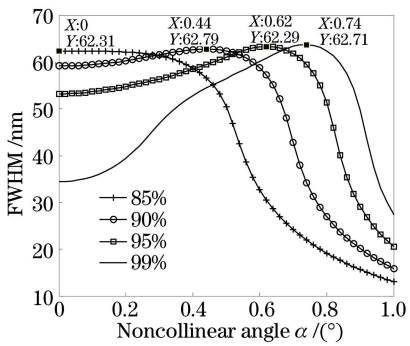

Fig. 5 FWHM of spectrum bandwidth versus noncollinear angle at four different deuteration levels, ZPMW is 808 nm

By inspecting Figs. 2(c) and (d), we approximate the phase-matching curve of the 99% deuteration level to a parabola in the vicinity of the extreme, and for different noncollinear angles α, the curve shape would not change significantly. This kind of phase-matching curve will always have two intersections with the zero mismatch line. There are possibilities that a much larger bandwidth can be obtained when we adjust the ZPMW to a shorter wavelength while the zero phase mismatch is at a longer wavelength, and a larger bandwidth can be obtained because the phase mismatch of those wavelengths around the two intersections is small. However, the gain around 808 nm will be greatly reduced if the phase mismatch is too big under this match geometry. Therefore, taking advantage of the noncollinear OPA geometry is necessary to make some compensation. Fig. 6 illustrates the FWHM of spectrum bandwidth at various noncollinear angles for different ZPMWs of 778 nm, 788 nm, and 798 nm, and these OPA bandwidth simulations are specific to the 99% deuteration level DKDP. The largest FWHM has reached 80 nm when the ZPMW is adjusted to 778 nm and the noncollinear angle is 0.7°. However, the spectrum in Fig. 7(a) shows that the energy gain of 808 nm is small (about 6) due to the large phase mismatch under this phase-matching condition, which will deteriorate the temporal profile of the output signal. Therefore, some better phase-matching settings are shown in Figs. 7(b) and (c), with the total gain of signal about 15 for both cases. It is noteworthy that there are some restrictions brought by the phase-matching cure. First, the zero phase mismatch wavelength should not be too short from the incident signal spectrum central wavelength 808 nm. It is not possible to obtain enough gain and broad bandwidth simultaneously. Figs. 7(a) and (d) present this contradiction. Second, setting the zero phase mismatch wavelength longer than 808 nm is useless in this method. As far as we are concerned, wavelengths between 778 nm and 790 nm are all appropriate, and for different wavelengths, the adaptive noncollinear angle should change as well. The most important thing is that the higher deuteration level is, the broader the wavelength adjustment range is, which is also the reason why we use the 99% deuteration level DKDP here.

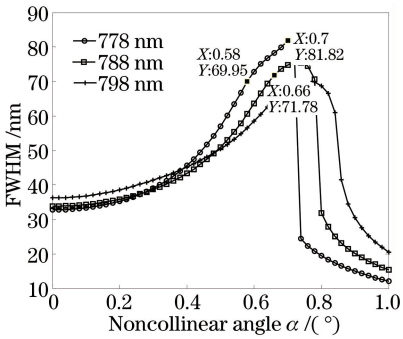

Fig. 6 FWHM of spectrum bandwidth versus noncollinear angle after adjusting the ZPMWs to 778 nm, 788 nm, and 798 nm

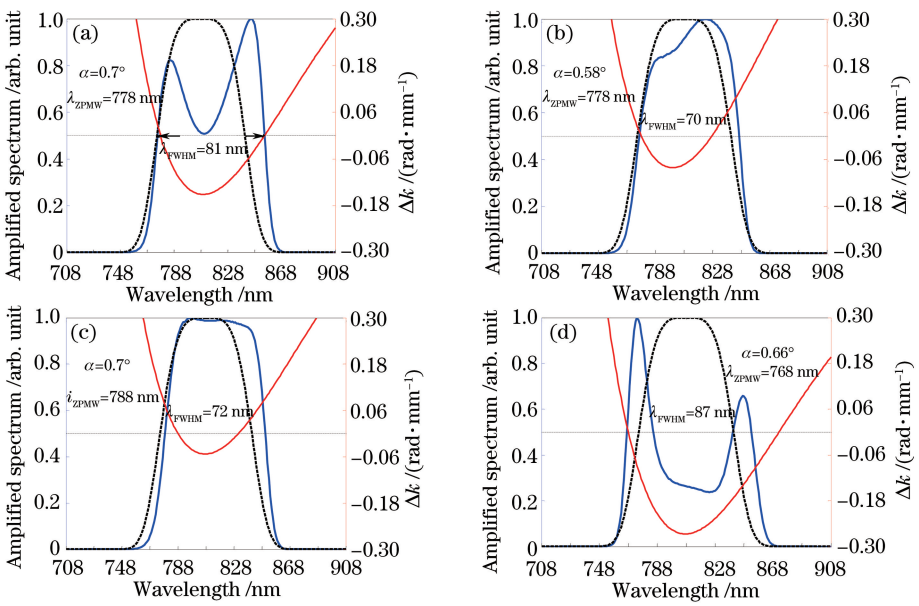

Fig. 7 Amplified signal spectra with different noncollinear angles after adjusting the ZPMWs to 768 nm, 778 nm, and 788 nm. The dotted black line is the incident signal spectrum, blue line is the amplified spectrum, and the red line is the phase-matching curve

Finally, we calculate the compression of amplified signal pulse in Figs. 7(a), (b), and (c). The results in Fig. 8 show that the spectrum of the FWHM can fulfill the compression near 20 fs.

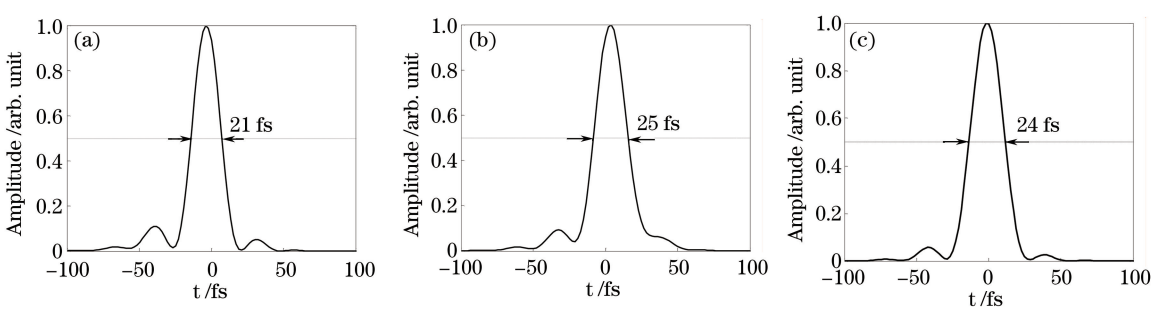

Fig. 8 Compression of amplified signal pulse. (a) In Fig. 7(a); (b) in Fig. 7(b); (c) in Fig. 7(c)

4 Conclusion

An ultra-intense, ultra-short laser amplification chain based on OPCPA is proposed with a 808-nm centered signal and a 526.5-nm pumped from SHG of Nd:glass laser. A considerably mature and stable Ti:sapphire front-end oscillator can be used to provide an ultra-broadband 808-nm centered signal seed. The LBO, YCOB, or BBO crystals can be used in the OPCPA with aperture smaller than 100 mm. However, as the energy is increased in the main OPA, the aperture of the crystal needs to be increased to prevent damage, limiting the choice of available crystals. Therefore, the DKDP is analyzed because its size can be grown to several hundred millimeters.

The nonlinear properties of DKDP crystal are highly sensitive to the degree of deuteration. From the study of the phase-matching curves, the parametric bandwidth is smaller than 20 nm when the deuteration level of DKDP is inferior to 85%. This cannot be used as the broad bandwidth 808-nm centered OPA nonlinear crystal in the last amplification stage of petawatt laser systems. The results are improved when the deuteration level is higher than 85%, as the parametric bandwidth can be larger than 70 nm when we adjust the noncollinear angle according to Figs. 2(c) and (d).

Meanwhile, the amplified signal spectrum from the main OPA is numerically simulated with the consideration of absorption. The impact of absorption on the conversion efficiency is small in our OPA structure. The decrease in conversion efficiency can be recovered when we lengthen the crystal. The widest amplified spectrum bandwidth for different deuteration levels is obtained with the best noncollinear angle and the ZPMW is set to 808 nm. The largest bandwidth is 66 nm when the noncollinear angle is adjusted to 0.76° in the 99% deuterated level DKDP, which is smaller than that of the incident signal spectrum. To obtain a larger bandwidth, we move the ZPMW to a shorter wavelength, such as 778 nm ZPMW and 788 nm ZPMW. The largest bandwidth has reached 81 nm at the 778 nm ZPMW case with the noncollinear angle of 0.64°. For a better amplified spectrum shape that has enough energy gain, the 778 nm ZPMW with the noncollinear angle of 0.58° and the 788 nm ZPMW with the noncollinear angle of 0.66° should be recommended.

In conclusion, DKDP crystal of the deuteration level higher than 90% can provide broad gain bandwidth and enough gain to support the final large-aperture optical parametric chirped pulse amplification systems centered at 808 nm.

Reference

1 Danson C, Hillier D, Hopps N, *et al*. Petawatt class lasers worldwide[J]. High Power Laser Science and Engineering, 2015, 3(1): 1-14.

2 Hernandez-Gomez C, Blake S P, Chekhlov O, *et al*. The Vulcan 10 PW project[C]. The Sixth International Conference on Inertial Fusion Sciences and Applications, 2010, 244: 032006.

3 Exawatt center for extreme light studies (XCELS) [EB/OL]. http://www.xcels.iapras.ru/img/site-XCELS.pdf.

4 Zuegel J D, Bank S W, Begishev I A, *et al*. Status of high-energy OPCPA at LLE and future prospects[C]. Conference on Lasers and Electro-Optics, 2014, JTh4L: JTh4L. 4.

5 Lozhkarev V V, Freidman G I, Ginzburg V N, *et al*. Study of broadband optical parametric chirped pulse amplification in a DKDP crystal pumped by the second harmonic of a Nd:YLF laser[J]. Laser Physics, 2005, 15(9): 1319-1333.

6 Skrobol C, Karsch S, Klingebiel S, *et al*. Broadband amplification by picosecond OPCPA in DKDP pumped at 515 nm [J]. Optics Express, 2012, 20(4): 4619-4629.

7 Akbari R, Major A. Optical, spectral and phase-matching properties of BIBO, BBO and LBO crystals for optical parametric oscillation in the visible and near-infrared wavelength ranges[J]. Laser Physics, 2013, 23(3): 035401.

8 Sun M, Ji L, Bi Q, *et al*. Analysis of ultra-broadband high-energy optical parametric chirped pulse amplifier based on YCOB crystal[J]. Chinese Optics Letters, 2011, 9(10): 101901.

9 Prandolini M J, Riedel R, Schulz M, *et al*. Design considerations for a high power, ultrabroadband optical parametric chirped-pulse amplifier[J]. Optics Express, 2014, 22(2): 1594-1607.

10 Zhao B Z, Jiang Y L, Sueda K, *et al*. Ultrabroadband noncollinear optical parametric amplification with LBO crystal[J]. Optics Express, 2008, 16(23): 18863-18868.

11 Novák O, Turčičová H, Smrž M, *et al*. Broadband femtosecond OPCPA system driven by the single-shot narrow-band iodine photodissociation laser SOFIA[J]. Applied Physics B, 2012, 108(3): 501-508.

12 Yu L H, Liang X Y, Li X R, *et al*. Optimization for high-energy and high-efficiency broadband optical parametric chirped-pulse amplification in LBO near 800 nm[J]. Optics Letters, 2015, 40(14): 3412-3415.

13 Yu L H, Liang X Y, Li X R, *et al*. Experimental demonstration of joule-level non-collinear optical parametric chirped-pulse amplification in yttrium calcium oxyborate[J]. Optics Letters, 2012, 37(10): 1712-1714.

14 Galimberti M, Hernandez-Gomez C, Musgrave I, *et al*. Influence of the deuteration level of the KD* P crystal on multi-PW class OPCPA laser[J]. Optics Communications, 2013, 309: 80-84.

15 Guo X , Xu Y, Zou X, *et al*. Non-collinear phase-matching geometries in optical parametric chirped-pulse amplification [J]. Optics Communications, 2014, 330: 24-29.

16 Baumgartner R A, Byer R L. Optical parametric amplification[J]. IEEE J Quantum Electron, 1979, 15(6): 432-444.